Short-Time Fourier Transform of Deeply Located Tunnel Signatures Measured by Cross-Borehole Pulse Radar

Sang-Wook Kim, Se-Yun Kim, *Member, IEEE*, and Sangwook Nam, *Member, IEEE*

Abstract—**The pulse signatures of a deeply located dormant tunnel are measured by operating cross-borehole short-pulse radar in a well-suited tunnel test site in Korea. The relatively fast arrival of the first peak at depth of the empty tunnel, as indicated by data analysis, may play a key role in detecting the tunnel's precise location. Following short-time Fourier transform (STFT) of the data, the arrival time of the first peak is shown to be faster and more distinctive than that without STFT if the observation frequency is properly selected.**

Index Terms—**Air cavity, cross-hole radar, pulse radar, short-time Fourier transform (STFT), underground tunnel.**

I. Introduction

ONE of the tantalizing problems in geophysical exploration has been the detection of deeply located dormant tunnels with about 2 m in diameter in Korea [1]. Recently, many efforts have been attempted to find a more effective detection method using electromagnetic waves [2], [3]. The relatively fast propagation of pulse signatures through the empty tunnel, using the cross-borehole pulse radar system, has been used to detect the tunnel's deeply located position [4]–[7]. The tunnel boundary causes severe attenuation, and multiple reflections inside tunnels distort the pulse signal shapes. Olhoeft [8], [9] investigated the characteristic features of the tunnel signature by extracting the first and second peaks of the received signal in time domain. The arrival time and amplitude of the first peak and the time delay of the second peak have been mainly used in the analysis of measured radar data because of the simplicity and accuracy of these parameters. The most important parameter is the time-of-peak (TOP), which denotes the arrival time of the first peak. However, underground rock is highly weathered, jointed, and fractured, and the TOP pattern extracted from the raw data is distorted due to the interference generated from fault, joint, lode, and underground water. Hence, it is important to enhance the fast arrival of the TOP in the depth of the tunnel.

In 2007, we developed a cross-borehole pulse radar system for hole-to-hole measurements of electromagnetic pulse propagation through underground rock [10]. This radar is used to measure and analyze the pulse signatures of a deeply located dormant tunnel in a well-suited tunnel test site in Korea [11], [12]. The TOP pattern, extracted from the measured raw data, illustrates the relatively fast arrival time in the depth of the tunnel. The conventional Fourier transform of the raw data shows that the spectral components at a swept frequency of 30–60 MHz are attenuated significantly due to the tunnel. This result agrees well with the fact that the data measured by the stepped-frequency continuous wave cross-borehole radar [13] suffer from severe attenuation in the depth of the tunnel if the swept frequency is adjusted to about 30–60 MHz. It leads us to consider the short-time Fourier transform (STFT) [14] of the raw data, which decomposes any specific frequency contribution from the broadband response signal at any instant in time. As an effective window function, Duff and Zook [15] applied the Wigner–Ville distribution to the pulsed electromagnetic search system data measured in another well-suited tunnel test site in Korea. Their results showed the characteristic features of the dormant tunnel in the time–frequency domain. Olhoeft [8] used fast Fourier transform (FFT) deconvolution to enhance the resolution of the weak signal. This method helps to search the first peak arrivals without any changes in time scale. Our interest is focused on finding a more effective technique to render the TOP patterns in the depth of the tunnel. In this letter, the STFT is applied to the raw data measured by our cross-borehole pulse radar. We show that the TOP patterns of the STFT components calculated at 40 and 50 MHz are enhanced significantly and are more distinct in the depth of the tunnel.

II. Measurement of Radar Data

Fig. 1 shows the 3-D geometry of a well-suited tunnel test site in Korea. The empty dormant tunnel, which has a cross section of 2 m by 2 m, is located at a depth of 72–74 m. The surrounding rock is granite with a relative permittivity of 5.8 from 63 to 83 m deep. The transmitter of the cross-borehole pulse radar is inserted into the left borehole Tx, and its receiver is operated inside the right borehole Rx. The oblique angle of the tunnel axis to the line of sight between the borehole pair in the same depth is 85.7°. The deviation of each borehole was measured by the deviation measurement system. The separation distance between the borehole pair is 14.3 m on the surface, but the separation distance increases gradually to 15.9, 16.3, and 16.8 m at a depth of 63, 73, and 83 m, respectively, as shown in Fig. 1. Both the transmitting and receiving antennas of the

Manuscript received January 7, 2010; revised May 3, 2010 and August 2, 2010; accepted October 7, 2010. This work was supported in part by the Korean Institute of Science and Technology under contract 2E21711.

S.-W. Kim and S. Nam are with the Society of Electrical Engineering and Computer Science, Seoul National University, Seoul 151-744, Korea (e-mail: swkim@acl.snu.ac.kr; snam@snu.ac.kr).

S.-Y. Kim is with the Imaging Media Research Center, Korea Institute of Science and Technology, Seoul 136-791, Korea (e-mail: ksy@imrc.kist.re.kr).

Digital Object Identifier 10.1109/LGRS.2010.2089039

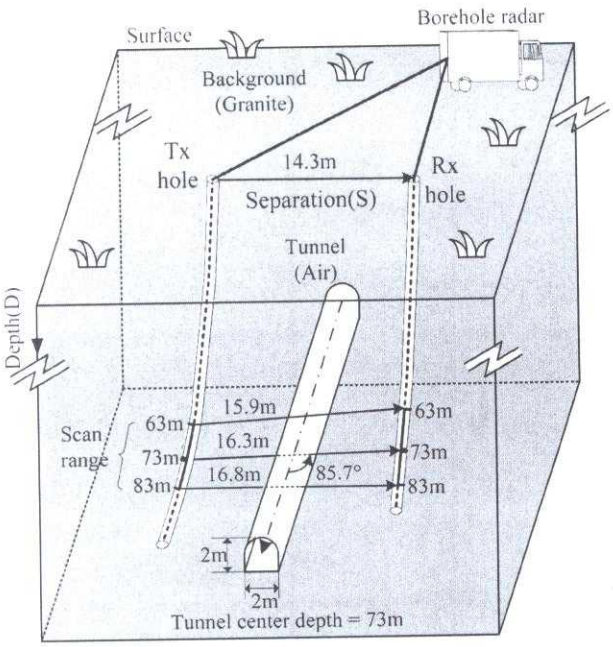

Fig. 1. Three-dimensional geometry of the well-suited tunnel test site.

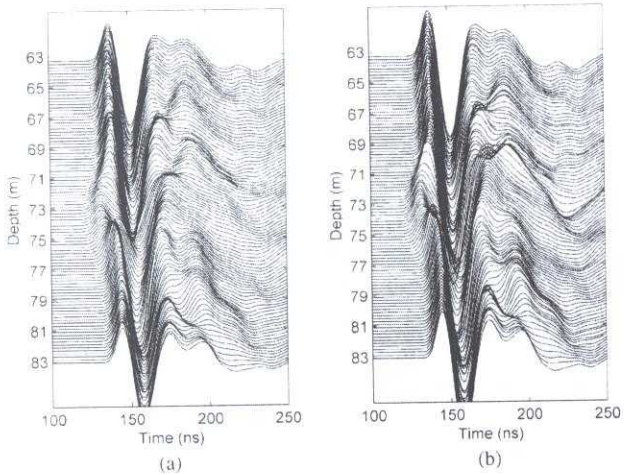

Fig. 2. Cross-borehole radar signatures measured from 83 to 63 m. (a) Original data and (b) normalized data.

cross-borehole pulse radar are the same form as the resistor-loaded cylindrical dipole with 1.5-m length. While the transmitting antenna radiated an electromagnetic pulse with 5-ns width at a depth from 83 to 63 m in the borehole Tx, the receiving antenna in the borehole Rx attempted to detect the pulse propagated through the man-made tunnel between the two boreholes, maintaining the same depth as the transmitter. Because this radar system is operated in various underground conditions, a wideband signal is more useful to cover these situations than a narrow specific band.

Fig. 2(a) illustrates the pulse signal patterns received at the scan depths from 83 to 63 m with the receiver in borehole Rx. As expected, the arrival of the first pulse peak revealed a relatively fast penetration through the tunnel. The amplitude of the first peak was significantly reduced around depths of the tunnel due to electromagnetic scattering by the empty tunnel.

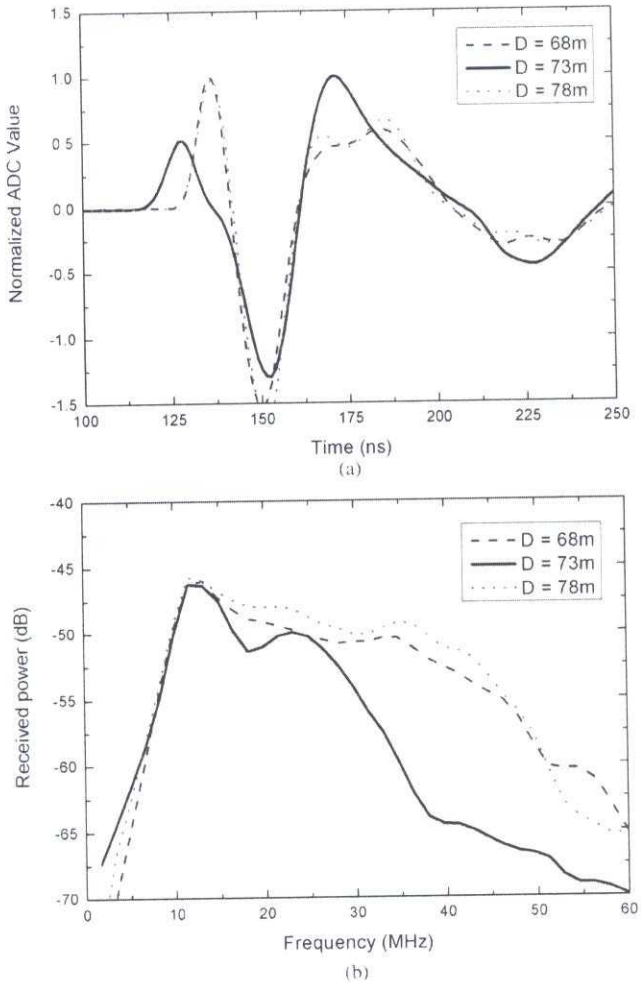

Fig. 3. Three signature patterns received at a depth of 68, 73, and 78 m. (a) Time domain and (b) spectral domain.

and the received pulse arrived faster as the receiver moves up due to the change in the separation distance between the two boreholes, as shown in Fig. 1. To enhance the recognition of the tunnel signature, the original data in Fig. 2(a) was normalized, as shown in Fig. 2(b), using the following process. First, the pulse signal measured at each depth was normalized by its maximum amplitude, thus preventing the strong attenuation of the tunnel signature from being concealed by other signals in the wiggle trace graph. Second, the gradual variation in arrival time due to the deviation of the involved boreholes was compensated by using the normal moveout process [16]. This process converts the data acquired at different separation distances into signatures measured at the same distance.

The normalized data shown in Fig. 2(b) were, from this point on, used as our raw data. Three received pulse patterns at 68, 73, and 78 m were extracted from the normalized data. The TOP at 73 m, as shown in Fig. 3(a), occurred relatively faster (by about 10 ns) than the TOP at 68 or 78 m. This fast arrival of the TOP at 73 m played a key role in precisely locating the empty tunnel. Applying the conventional Fourier transform to the pulse patterns, we obtained the spectral patterns shown in Fig. 3(b). Compared to the spectral patterns at 68 and 78 m, the

spectral pattern at 73 m suffered from significant attenuation in the range between 30 and 60 MHz. Although spectral patterns have large amplitudes in the band of 30 MHz below, there is no significant difference between amplitude patterns with and without the tunnel. The strong attenuation above 60 MHz due to the high lossy and inhomogeneous property of the surrounding rock around the tunnel caused noise contamination of the corresponding spectral components. Hence, the limited frequency band may effectively enhance the distinction of the tunnel signature in the received signal pattern. To separate the effective spectral components from the raw data in Fig. 3(b), we performed STFT, as described in the next section.

III. STFT of Radar Data

Consider the received signature $r(n, D)$, which is generated by sampling the raw data at a discrete time $n\Delta t$ at depth D. The STFT component of $r(n, D)$ at frequency f_0 is represented by

$$R_{f_0}(m, D) = \sum_{n=0}^{N} r(n, D) W_M(n - m) e^{-j2\pi f_0 n \Delta t} \quad (1)$$

where N is the total number of the time domain sampling and $W_M(n)$ is a discrete window function. For simplicity, we use the Hanning window function with the window size M [9] as

$$W_M(n) = 0.5\left(1 + \cos\left(\frac{2n}{M}\pi\right)\right), \quad n = -\frac{M}{2}, \ldots, -1, 0, 1, \ldots, \frac{M}{2}. \quad (2)$$

The width M in (2) plays a key role in determining the resolution in time domain and limiting the width of interesting band in frequency domain. If the window size shrinks extremely, the result of STFT method approaches to the raw data. Conversely, if the window size expands infinitely, it becomes the coefficient of FFT at the center frequency. In this paper, M of 120 time steps is determined to get the optimal performance of our measured data. The coefficients of the STFT are calculated by performing the discrete Fourier transform after shifting the window function by m time step at every receiver point D and specific frequency f_0 using (1).

Fig. 4(a)–(d) illustrates the amplitude of the STFT components at 20, 30, 40, and 50 MHz, respectively. These amplitudes are normalized by the maximum amplitude at every depth. The bandpass filter (BPF) property of the STFT comprehensively shows the different behavior of four frequency components. In the low-frequency bands of 20 and 30 MHz, a strong tunnel signature cannot be identified in Fig. 4(a) and (b), respectively. This result implies that low-frequency components pass through the tunnel without any scattering because of low resolution. In contrast, strong scattering in the high-frequency components results in double peaks, and the first peaks are highly accelerated around depths of the tunnel, as shown in Fig. 4(c) and (d).

Fig. 5 shows the TOP patterns extracted from the STFT components in Fig. 4 and raw data in Fig. 2(b). Because the absolute values of the extracted TOP patterns are appeared at different delay time, they are not suitable to investigate the effect of STFT on TOP variation. This led us to normalize the absolute TOP patterns as follows: 1) For each TOP pattern, the straight line connecting two TOP values at 63 and 83 m

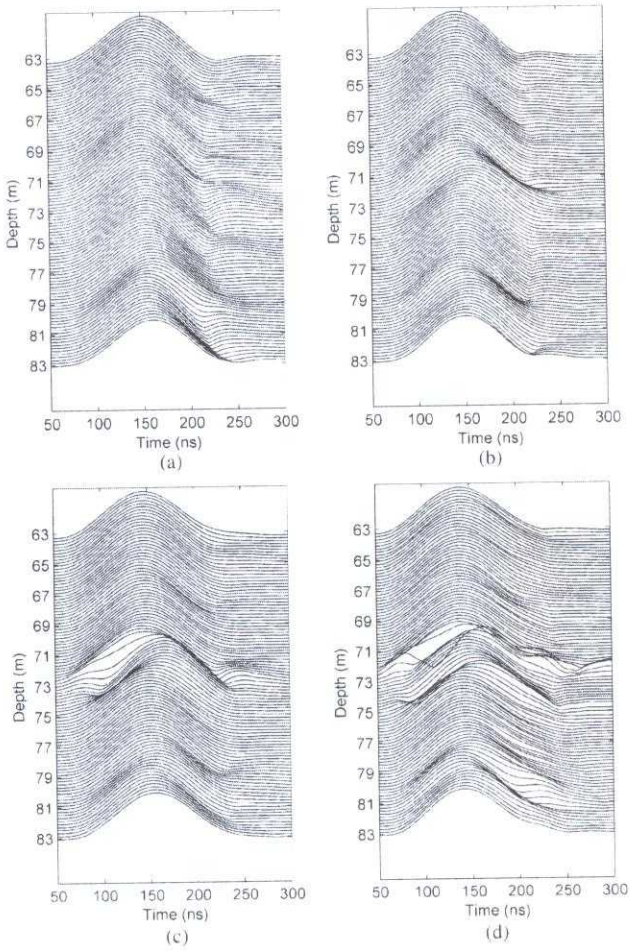

Fig. 4. Time domain responses of the STFT components when Hanning window size (M) is 120. (a) 20, (b) 30, (c) 40, and (d) 50 MHz.

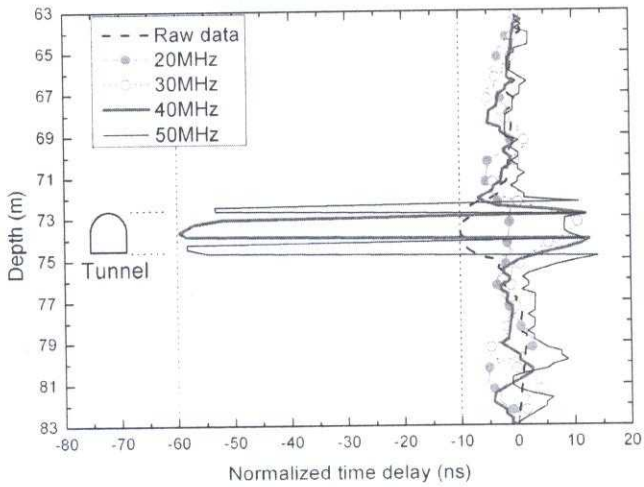

Fig. 5. Comparison of four TOP patterns extracted from the STFT components in Fig. 4 with that of the raw data in Fig. 2(b).

was constructed as a linear approximation of the TOP pattern in cases where the tunnel at 73 m disappeared. 2) The normalized TOP was obtained by extracting the absolute TOP with the tunnel from the straight-line TOP without the tunnel. Then, one may expect the existence of an empty tunnel to be easily recognized by simply searching for the fast arrival region in the normalized TOP pattern. Compared to the TOP pattern extracted from the raw data in Fig. 2(b), the normalized delay time of the components at 40 and 50 MHz is decreased from -10 to -60 ns. Although the TOP pattern of the 40-MHz component is accelerated around the tunnel center, the acceleration of the TOP pattern at 50 MHz can be identified at the top and bottom boundary of the tunnel. This result indicates that the TOP pattern extracted from the STFT components at some specific frequencies may enhance the capability of our cross-borehole pulse radar in the detection of deeply located dormant tunnels.

In the frequency-swept cross-borehole radar [17], the scattered field from an empty tunnel became out of phase in comparison with the incident field when the half-wavelength of the incident field in the rock was close to the diameter of the tunnel. It rendered the significant attenuation to occur at the top and bottom boundaries of the tunnel. In the background medium of our measurement site, the half-wavelength of 40 MHz is about 2 m. Hence, about 40 MHz, the amplitude of the total field is attenuated significantly at the horizontal position of the tunnel, as shown in Fig. 3(b). This particular scattering phenomenon makes it possible to accelerate the TOP only by applying the STFT method, as shown in Fig. 5.

IV. Conclusion

The cross-borehole pulse radar signatures of a deeply located dormant tunnel were measured in a well-suited tunnel test site in Korea. The relatively fast arrival of the first peak at depth in the empty tunnel was enhanced by applying STFT to the radar data. We clearly showed that the TOP patterns of the STFT components at 40 and 50 MHz are faster and more distinctive than that of the raw data.

The time acceleration of 10–13 ns due to the air-filled tunnel is somewhat small in comparison with the variation of the first arrival time due to the inhomogeneous property of the surrounding rock. In our approach, the first arrival time was amplified in the tunnel region using the property of zooming in the STFT method. It is accomplished by eliminating not only the lower frequency components containing no tunnel signature but also the higher frequency components attenuating significantly below noise level. We believe that the bandpass filtering property of the STFT scheme would be very effective tool for detecting the tunnel in highly inhomogeneous rock.

References

[1] B. Duff, "A review of electromagnetic methods used for detection of underground tunnels and cavities," in *Proc. IEEE Int. Symp. Antennas Propag.*, 1983, vol. 21, pp. 634–638.

[2] T. Takayama and M. Sato, "A novel direction-finding algorithm for directional borehole radar," *IEEE Trans. Geosci. Remote Sens.*, vol. 45, no. 8, pp. 2520–2528, Aug. 2007.

[3] L. Lo Monte, D. Erricolo, F. Soldovieri, and M. C. Wicks, "Radio frequency tomography for tunnel detection," *IEEE Trans. Geosci. Remote Sens.*, vol. 48, no. 3, pp. 1128–1137, Mar. 2010.

[4] M. L. Moran and R. J. Greenfield, "Radar signature of a 2.5-D tunnel," *Geophysics*, vol. 58, no. 11, pp. 1573–1587, Nov. 1993.

[5] J. Schneider and I. C. Peden, "Detection of tunnels in low loss media illuminated by a transient pulse," *IEEE Trans. Geosci. Remote Sens.*, vol. 31, no. 2, pp. 503–506, Mar. 1993.

[6] H. Zhou and M. Sato, "Subsurface cavity imaging by cross borehole radar measurements," *IEEE Trans. Geosci. Remote Sens.*, vol. 42, no. 2, pp. 335–341, Feb. 2004.

[7] K. Takahashi and M. Sato, "Parametric inversion technique for location of cylindrical structures by cross-hole measurements," *IEEE Trans. Geosci. Remote Sens.*, vol. 44, no. 11, pp. 3348–3355, Nov. 2006.

[8] G. R. Olhoeft, "Interpretation of hole-to-hole radar measurements," in *Proc. 3rd Tech. Symp. Tunnel Detection*, Golden, CO, 1988, pp. 617–629.

[9] G. R. Olhoeft, "Velocity, attenuation, dispersion and diffraction hole-to-hole radar," in *Proc. 4th Tunnel Detection Symp. Subsurface Exploration Technol.*, Golden, CO, 1993, pp. 308–320.

[10] S. W. Kim, S. Y. Hyun, J.-H. Lee, S.-Y. Lee, J.-H. Cho, K.-T. Oh, and S.-Y. Kim, "The development of a pulse borehole radar system for underground cavity detection," in *Proc. IEICE Tech. Rep. SANE2007-80 9th Workshop Subsurface Electromagn. Meas.*, Seoul, South Korea, 2007, pp. 93–97.

[11] S. W. Kim and S. Y. Kim, "Analysis of cross-borehole pulse radar signatures measured at various tunnel angle," *Explor. Geophys.*, vol. 41, no. 1, pp. 96–101, Feb. 2010.

[12] S. W. Kim, S. Y. Kim, and S. Nam, "Estimation of the penetration angle of a man-made tunnel using time of arrival measured by short-pulse cross-borehole radar," *Geophysics*, vol. 75, no. 3, pp. J11–J18, May/Jun. 2010.

[13] S. Y. Kim and J. W. Ra, "The role of cross borehole radar in the discovery of fourth tunnel at Korea DMZ," in *Proc. 4th Tunnel Detection Symp. Subsurface Explor. Technol.*, Golden, CO, 1993, pp. 253–257.

[14] F. J. Harris, "On the use of windows for harmonic analysis with the discrete Fourier transform," *Proc. IEEE*, vol. 66, no. 1, pp. 51–83, Jan. 1978.

[15] B. M. Duff and B. J. Zook, "Time-frequency representations applied to analysis of hole-to-hole electromagnetic data," in *Proc. 4th Tunnel Detection Symp. Subsurface Exploration Technol.*, Golden, CO, 1993, pp. 221–252.

[16] M. Sato and X. Feng, "GPR migration algorithm for landmines buried in inhomogeneous soil," in *Proc. IEEE Int. Symp. Antennas Propag.*, 2005, vol. 1B, pp. 206–209.

[17] T. K. Lee, S. O. Park, S.-Y. Kim, and J. W. Ra, "Near-field diffraction pattern by an underground void of circular cylinder," *Microw. Opt. Technol. Lett.*, vol. 2, no. 5, pp. 179–183, May 1989.